Application of Thermoset Polymer Coating with Ceramic Particle to Additively Manufactured Carbon Fiber Reinforced Thermoplastic Composite Tooling

Garam Kim, Eduardo Barocio

Abstract

A thermoset polymer liquid coating reinforced with ceramic particles was applied on the surface of an additively manufactured carbon fiber-reinforced thermoplastic composites to improve its surface characteristics for composite tooling application. The tool demonstrated herein was fabricated via material extrusion additive manufacturing (MEAM) and served for the fabrication of autoclave-cured laminated composite structures. Test specimens used in this investigation were additively manufactured with Polyphenylene Sulfide (PPS) reinforced with 50% by weight of carbon fiber. Approximately 10 μm thick thermoset resin-based coating reinforced with ceramic particles was applied on the surface of flat specimens using the liquid spray coating technique and cured at an elevated temperature. Surface characteristics relevant to molds used in composite manufacturing such as surface roughness, abrasion resistance, hardness, friction, and vacuum integrity were assessed for the coated and noncoated specimens. Autoclave composite part manufacturing tools were built and coated to study demolding property of the coated tool throughout multiple autoclave cycles. The result showed that the coating improved abrasion resistance, vacuum integrity, demolding property, and lowered surface friction.

1. Introduction

The use of fiber reinforced composite materials in applications within the aerospace, automobile, maritime, and sporting goods industries has increased rapidly due to favorable physical and mechanical properties of the material such as high strength to density ratio [1,2]. Molds are essential for the fabrication of composite parts since it provides the geometrical shape and the surface finish of the composite part [3–5]. Molds are often made from aluminum, steel, tooling board, or composite materials similar to the part being produced with the mold [2,5]. Among these, composite molds are gaining more attention due to the low-weight, low coefficient of thermal expansion (CTE), and temperature stability [5,6]. Further, composite molds offer the potential of tailoring the CTE of the mold according to the CTE of the part being fabricated. Traditionally, composite tools are handmade by operators, and therefore the quality of the tool can vary depending on the skills of the operator [7,8]. Further, handmade composite tools are labor and time intensive, and dimensional accuracy of the tool may not be guaranteed [7,8]. Especially, large-scale tools have several manufacturing steps which induces labor intensity to the tool manufacturing process [9]. To overcome these issues, the newly emerging fiber reinforced composite additive manufacturing technology is often used for composite tool manufacturing process [7,8,10].

Additive manufacturing composite material is a promising technology for mold manufacturing because it reduces cost, time, and labor to make a composite mold [8,11]. However, the newly emerged additively manufactured fiber reinforced composite molds for composite part

manufacturing have showed some limitations to achieve a high-performance mold surface. Dimensional accuracy requirements still demands machining of the near-net-shape additively manufactured molds [12,13]. The surface of the additively manufactured fiber reinforced composite mold is not as durable as a traditional metal mold [6]. Therefore, it is more prone to scratches, nicks, or dents during the composite part manufacturing process [6,8,12,14]. Further, during the machining process, surface irregularities can develop due to fiber breakage, fiber pull-out, matrix cracking, and overheating of the polymer by friction [15]. Surface defects can lead to variations in roughness at the surface of the tool which is transferred to the surface of the composite part produced with the tool [14,15]. The roughness on the surface of the tool can promote mechanical interlocking between the part and the tool, thereby increasing the force required to release the part from the tool [7]. Excessive demolding forces can damage the tool, the part, or both during the part demolding process [16,17]. Also, the bead-by-bead additive manufacturing process can leave gaps between adjacent beads which can serve as air pathways, thereby compromising the vacuum integrity of the mold which is detrimental for the consolidation of a laminated composite structure produced with the mold [14,18].

For these reasons, an additional coating on the additively manufactured mold is often used [19]. Gelcoat is one of the most common coating materials that is applied on fiber reinforced composite mold to improve its surface quality [20]. Gelcoat is approximately 0.406 - 0.508 mm thick, and it is generally applied via liquid spray. The gelcoat can provide a durable and smooth surface while protecting the substrate from the environment [19–21]. Gelcoats can be based on a thermoset resin, such as epoxy or polyester, modified to be able to spray for application [20]. Further, additives can be incorporated into the liquid resin coating to provide additional functionalities [21–23] such as wear resistance, electrical conductivity, and flame resistance. This work investigates the changes to the surface characteristics of an additively manufactured material upon the application of a thermoset resin-based coating reinforced with ceramic particles. More specifically, this study focuses on the surface characteristics relevant to molds used in the fabrication of composite parts including surface hardness, abrasion resistance, surface roughness, surface friction, vacuum integrity, and demolding force. Test specimens were additively manufactured with 50% by weight of carbon fiber reinforced Polyphenylene Sulfide (PPS). A commercially available thin film liquid coating with ceramic particles (Cerakote E-series) was applied on the test specimen. Various surface properties, such as hardness, abrasion resistance, roughness, surface friction, and vacuum integrity of the coated surface were performed, and the results were compared to the pristine (non-coated) surface. The goal of this study was not only investigating surface properties of one coated surface but also introducing different surface property tests that were required for composite part manufacturing mold surface. The details of testing process and test result analysis for each test were demonstrated.

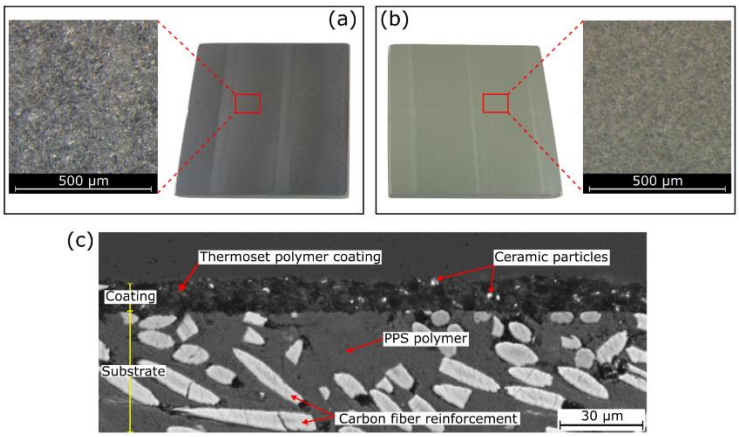

Figure 1. Stereoscopic image of the (a) non-coated and (b) coated test specimen. (c) Microscopic image of cross-sectional area of the coating applied on the substrate.

2. Methodology

2.1 Surface hardness test

Composite part manufacturing mold are often exposed to surface damage, such as scratch, nick, or dent during its service. The surface with high hardness is required to maximize the number of production run for composite part manufacturing mold. The surface hardness of the coated additively manufactured carbon fiber reinforced PPS composite test specimen was tested using a Barcol impressor in accordance with ASTM D2583, the test method for indentation hardness of rigid plastics by means of a Barcol impressor [24]. Barcol hardness test was a static hardness test which used an impressor to indent the surface of the material with a specific load. The depth of the indent was measured to determine the hardness level of the material surface. Qualitest GYZJ-934-1 was used for a Barcol impressor.

2.3 Surface roughness test

The surface roughness of the composite part manufacturing mold is an important factor that determined the surface finish quality and surface friction of the mold. The surface finish quality of the composite part and required demolding force are influenced by the surface roughness of the mold [3,4]. Therefore, low surface roughness is required for the mold surface. The surface roughness test was performed in accordance with ASTM D7127, standard test method for measurement of surface roughness of abrasive blast cleaned metal surfaces using a portable stylus instrument [25]. The Mitutoyo surf tester SJ-210 was used for the surface roughness test. In this study, arithmetical mean roughness (Ra) was used to compare the surface roughness level of the test specimen. The roughness was measured in the direction as same as machining direction.

2.2 Surface abrasion resistance

The rubbing action between the part and the mold during the repeated demolding process can cause frictional wear on the mold surface [26]. The repeated frictional wear can lead to deteriorate of mold surface characteristics and dimensional accuracy. Therefore, high surface abrasion resistance is required for composite part manufacturing mold surface. The surface

abrasion resistance test was performed in accordance with ASTM D4060, standard test method for abrasion resistance of organic coatings by the Taber abraser [27]. A Teledyne Taber abraser model 503 was used for an abrasion tester as shown in Figure 2(a). The abrasion resistance test specimen was mounted on the turntable, and two Taber abrasion wheels were placed on the top surface of the test specimen. The abrasion test was performed with two CS-10 Calibrase resilient wheels. When the turntable rotated, the abrasion wheels were rotated driven by the rotation of the test specimen. The rub-wear action between the test specimen and the abrasion wheels abraded the surface of the test specimen as shown in Figure 2(b). The vacuum system cleaned abraded particles on the test specimen during the test. The weight change of the test specimen corresponding to the number of abrasion cycles was used to compare surface abrasion resistance of the test specimen.

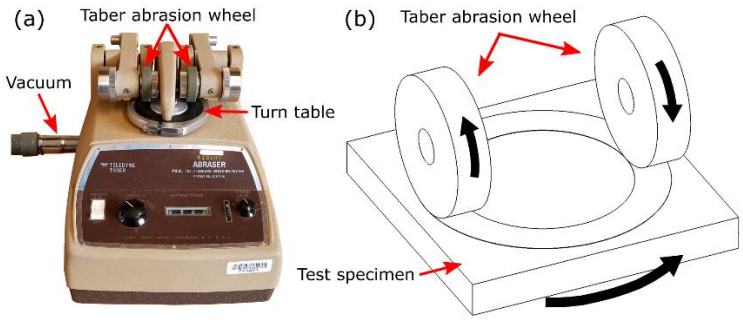

Figure 2. (a) Taber surface abrasion resistance tester and (b) schematic drawing of the surface abrading process during the surface abrasion resistance test.

2.4 Surface friction

In composite part manufacturing process, a cured composite part is demolded from the composite part manufacturing mold, and surface friction between the mold surface and the part affects required demolding force [28]. Therefore, low surface friction between composite part manufacturing mold surface and the part is preferred. To investigate how additional coating affected surface friction of the additively manufactured composite, a surface friction test was performed. Surface friction testing fixture which had flat plate and pulley which along the vertical axis of a MTS testing system was prepared. A carbon fiber composite laminate was installed on the top of the surface friction test plate and the test specimen was placed on the top of the carbon fiber composite laminate and connected to a 22.68 kg capacity load cell on the MTS machine with string through the pulley. A 6.26 kg of weight was placed on the top of the test specimen to apply normal force during the surface friction test and 50 mm/min of the pulling rate was used during the test. Figure 3(a) shows the surface friction test settings.

2.5 Vacuum integrity

In the composite part manufacturing process, sealed surface of the mold is important. During the composite part curing process, vacuum bag is often installed on the mold surface to apply pressure and consolidate the composite part [2,5]. If there is an air leak on the mold surface, it is difficult to achieve enough pressure applied to the part during the cure cycle [2,5]. To investigate how additional coating affects vacuum integrity of the additively manufactured fiber reinforced composite, vacuum integrity test was performed before and after the coating accordance to ASTM D5687, standard guide for preparation of flat composite panels with processing

guidelines for specimen preparation [29]. Vacuum bag was installed on the surface of the test specimen and about 84.66 kPa of vacuum pressure was applied. A vacuum pressure gauge was used to measure vacuum loss for 30 seconds. Each surface was tested 3 times. After all non-coated surface was tested, the coating was applied to the test specimen on both side and the vacuum integrity of the coated test specimen was tested same way 3 times. Figure 3(b) shows a picture of vacuum integrity test on the test specimen with a vacuum pressure gauge.

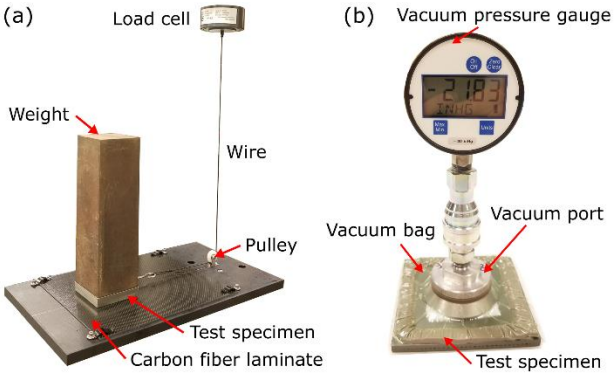

Figure 3. Test setting for the (a) surface friction test and (b) vacuum integrity test.

2.6 Demolding test

An experimental procedure was developed to investigate the effects of the coating on the demolding characteristics of printed composite tools. To quantify the effects of the coating on the demolding force, a tool geometry was designed to promote a demolding force resulting from the friction between the part and the tool. Figure 4(a) shows the cross-section of the tool for a cylindrical shape designed for the experiments used for characterizing the demolding force. A composite prepreg material was laid at the top and sides of the tool. When the composite material was cured in an elevated temperature and cooled down, the composite material shrank and generated normal force against the tool. During the demolding process, the sliding composite part on the tool applied a frictional shear stress between the tool and the part. The demolding test tool had a part ejecting system which had an ejector pin hole all the way through the tool, so the cured part could be demolded by pushing the ejector pin through the ejector pin hole.

Since the authors wanted to have a high demolding force of the tool during the demolding test, the authors used a woven fiber glass reinforced composite prepreg, which had a higher coefficient of thermal expansion (CTE) than carbon fiber, for the composite layup plies to increase the demolding force intentionally. Eight plies were laid on the surface of the tool following the stacking sequence $[0/45/30/60]_2$ which was designed to distribute the darts uniformly along the perimeter of the tool. An additional set of eight circular plies were applied at the top of the tool to reinforce the top face of the cylinder which was used for transferring the demolding force from the ejector pin to the part as shown in Figure 4(b-4). Following the application of the composite plies on the surface of the tool, the tool and part were enclosed under vacuum in a bag and prepared for an autoclave cure (180°C for two hours and under 586 kPa of external pressure). Figure 4(b) shows the prepreg layup process on the demolding test tool.

After the composite part was cured, the tool was installed in an MTS universal testing machine for the demolding test. The tool was flipped upside down and placed on the 88.9 mm diameter

aluminum support cylindrical tube, and an ejector pin was inserted from the bottom of the tool. The MTS testing system was set to compression test with a displacement change of 2 mm/min and 10 displacement and load data were recorded per second. The demolding test was completed and stopped when the composite part was fully demolded from the tool. Figure 4(c) shows the demolding test setting in MTS system. The load and displacement data were exported and analyzed. Each tool was used in 10 production cycles.

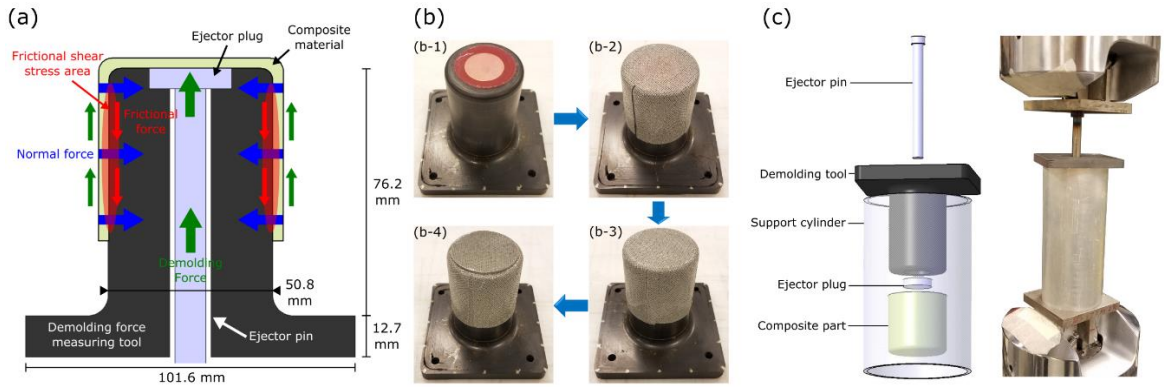

Figure 4. (a) The design of the demolding test tool and schematic drawing of applied forces between the tool and part during the demolding process. (b) Fiber glass reinforced composite prepreg material layup process on the demolding test tool; (b-1) a piece of solid release film on the top of the tool before 1st ply layup, (b-2) after 1st ply layup, (b-3) after 8th ply layup, and (b-4) after additional eight circle plies layup. (c) Schematic drawing of the demolding test setting and the demolding test setting in the MTS system.

3. Results

3.1 Hardness result

Four composite test specimens were prepared; two non-coated and two coated composite test specimens. 50 different surface hardness measurements from each test specimen, In addition, the surface hardness level of an aluminum 6061-T6 and a 1020 steel, which were commonly used metal for mold manufacturing, were measured to compare the hardness of the additively manufactured carbon fiber reinforced PPS composite to the hardness of a traditional metal. The average Barcol hardness of the coated composite specimen was 17.37 and the average Barcol hardness of the non-coated composite specimen was 22.67. The average Barcol of the coated test specimens was 23.38% lower than the non-coated test specimen. The average Barcol hardness of the aluminum and steel test specimen was significantly higher than the composite test specimens (aluminum = 79.80, steel = 89.62). Figure 5(a) shows a bar graph of the average Barcol hardness of each test specimen group with standard deviation bar.

3.2 Roughness result

Two non-coated and two coated composite test specimens were prepared. For each test specimen, 20 roughness measurements were collected. The roughness test results showed that the average Ra of the coated test specimens was 0.95, and the average Ra of the non-coated test specimens was 0.90. The coated composite test specimen had a 4.93% higher average Ra than

the non-coated composite test specimen. Figure 5(b) shows bar graph of the average Ra of the non-coated and coated composite test specimen with standard deviation bar.

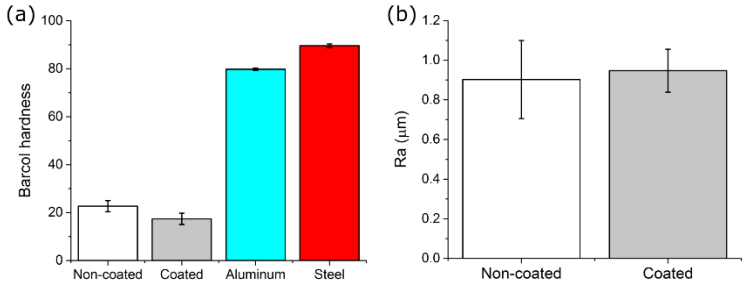

Figure 5. (a) Bar graph of average Barcol hardness with standard deviation bar for each test specimen; the non-coated, coated, aluminum, and steel test specimen. (c) Bar graph of the average Ra of the non-coated and coated composite test specimen with standard deviation bar.

3.3 Abrasion result

Taber wear index, which represented the rate of wear, for each test specimen was calculated and compared. The Taber wear index was calculated using the following equation [27];

$$I = [(w_a - w_b) \times 1000] \,/\, c$$

where I represents Taber wear index, w_a is the weight of the test specimen before abrasion, w_b is weight of the test specimen after abrasion, and c is the number of abrasion cycles. One non-coated and one coated composite abrasion resistance test specimen were tested, and 10 wear index were calculated from each test specimen. In addition, aluminum 6061-T6 and 1020 steel test specimen were tested to compare the wear index of the coated and non-coated additively manufactured carbon fiber reinforced PPS composite to the wear index of traditional metal. Figure 6(a) shows the weight change of each test specimen for every 200 abrasion cycles during the abrasion resistance test, and Figure 6(b) shows bar graph of the average wear index of each test specimen with standard deviation bar. The test results showed that the weight change of all test specimen had a linearly decreasing pattern. The results showed that the average wear index of the non-coated composite test specimens was 23.5, and the average wear index of coated composite test specimens was 2.5. The average wear index of the coated composite test specimens was 89.36% lower than the non-coated composite test specimen. Also, the average wear index of the coated composite test specimen was even lower than the average wear index of the aluminum (wear index = 7.5) and steel test specimen (wear index = 7).

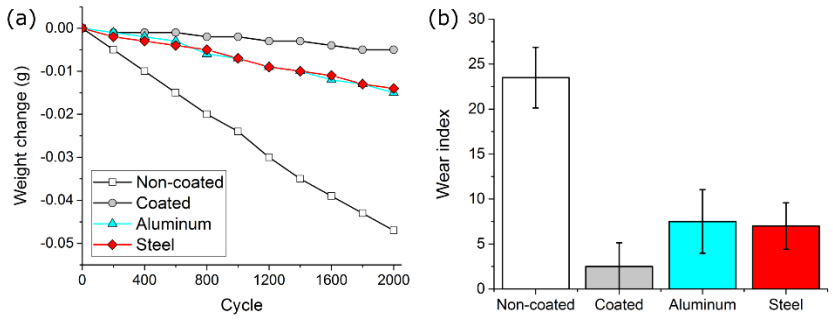

Figure 6. (a) The weight change of each test specimen for every 200 abrasion cycles during the abrasion resistance test. (b) The bar graph of the average wear index of each test specimen with standard deviation bar.

3.4 Surface friction result

10 non-coated and 10 coated test specimens were prepared and tested. Figure 7(a) shows the force versus displacement plot of the non-coated and coated test specimens during the friction test. The static and kinetic friction coefficient between the test specimen and the carbon fiber composite laminate were calculated using following equations;

$$F_s = \mu_s N$$
$$F_k = \mu_k N$$

Where F_s and F_k are static and kinetic friction force and μ_s and μ_k are static and kinetic friction coefficient. N is normal force applied to the test specimen during the test. The surface friction test result showed that the average static friction coefficient of the non-coated test specimen was 0.27, and the average static friction coefficient of the coated test specimen was 0.16. The average static friction coefficient of the coated test specimen was 40.16% lower than the average static friction coefficient of the non-coated test specimen as shown in Figure 7(b). Also, the average kinetic friction coefficient of the average kinetic friction coefficient of the non-coated test specimen was 0.24, and the coated test specimen was 0.15. The average kinetic friction coefficient of the coated test specimen was 38.37% lower than the average kinetic friction coefficient of the non-coated test specimen as shown in Figure 7(c).

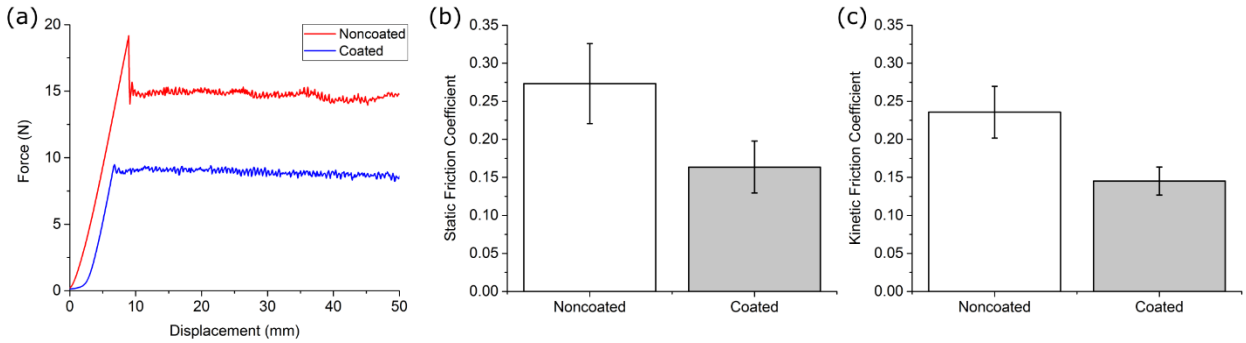

Figure 7. (a) Force versus displacement plot of surface friction test for one of the non-coated and coated test specimens. Bar graph of the average (b) static and (c) kinetic friction coefficient of the non-coated and coated test specimen with standard deviation bar.

3.5 Vacuum integrity results

8 non-coated vacuum integrity test specimens were prepared, and both sides of the test specimen were tested. In total, vacuum integrity of 16 surfaces were tested. The vacuum integrity test result showed different amount of vacuum loss for each test specimen. All non-coated test specimen had no more than 1.5 kPa vacuum loss for 30 seconds (ASTMD 5687 vacuum loss limit) except one surface had average of 4.206 kPa of vacuum loss. After the coating was applied, the vacuum loss for all test specimens was significantly reduced. Especially, the one surface which had average of 4.206 kPa vacuum loss had only average of 0.028 kPa of vacuum leak for 30 seconds after the coating was applied. Overall, the average vacuum loss for the test

specimen (M = 0.597, SD = 1.394) was decreased by 94.71% after the coating was applied (M = 0.032, SD = 0.013).

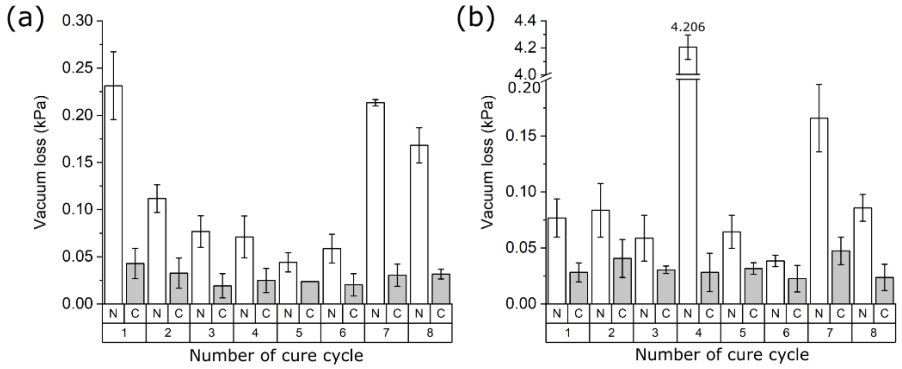

Figure 8. (a) Average vacuum loss for the test specimen side A with standard deviation bar, and (b) average vacuum loss for the test specimen side B with standard deviation bar. N represents the non-coated test specimen and C represents the coated test specimen.

3.6 Demolding result

Under the theory of surface friction, the demolding test data could be divided into two regions; static region, and kinetic region [30,31]. In the static region, the demolding force was applied to part, but the part did not start to be demolded from the tool yet due to the static friction and cohesion behavior between the cured part and the tool. The force continued increasing until it reached to the maximum demolding force [32]. After the maximum demolding force was reached, the force-displacement behavior transitioned from being controlled by the static friction to being controlled by the kinetic friction developed between the tool and the part [33]. Figure 4(a) shows the load versus displacement plot during the demolding test for the non-coated and coated tool (production cycle 1) with static and kinetic regions. The demolding force of the non-coated tool after about 10 mm displacement had severe load fluctuation. Therefore, the kinetic region of both demolding test data was filtered using an adjacent-averaging method with a window of 300 data points. Figures 4(b)-(c) showed the filtered load-displacement response for each of the 10 production cycles carried out with the non-coated and coated tool.

f_{max} is the maximum demolding force applied to the part during the demolding process. f_{max} is an important parameter for the tool because high f_{max} could lead to damaging either the tool or the part during the part demolding process. The average f_{max} of the coated tool ($f_{max,c}$) for the 10 production cycles was approximately 53.2% lower than the average f_{max} of the non-coated tool ($f_{max,n}$) for the 10 production cycles. At a given displacement value, the ratio of the kinetic friction coefficient of the non-coated and coated tool should be equal to the ratio of the corresponding demolding forces. The demolding property of the coated and non-coated tool in the kinetic region (kinetic friction coefficient) could be compared by comparing slope of the load versus displacement curve of the test specimens in the kinetic region. The average kinetic friction coefficient of the coated tool ($f_{k,c}$) was about 46% lower than the average kinetic friction coefficient of the non-coated tool ($f_{k,n}$).

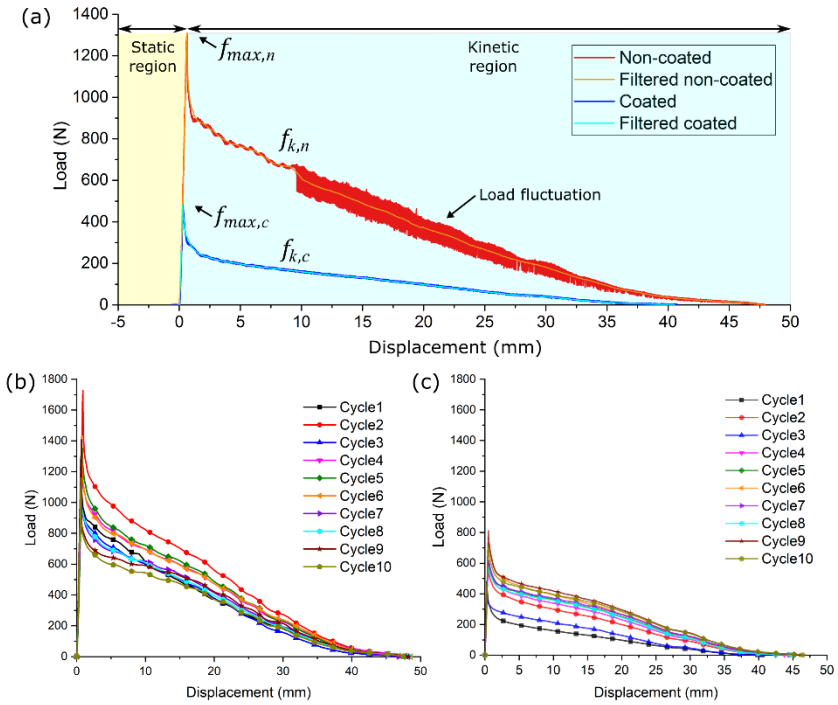

Figure 4. (a) Static and kinetic region in the load versus displacement plot during the demolding test for the non-coated and coated tool (production cycle 1) with markings of maximum demolding force of non-coated tool ($f_{max,n}$) and the coated tool ($f_{max,c}$) and kinetic friction force of the non-coated tool ($f_{k,n}$) and the coated tool ($f_{k,c}$). Load versus displacement data processed through an adjacent-averaging filter with a window size of 300 in the kinetic region for the (b) non-coated and the (c) coated tools during the demolding tests (cycle 1-10).

4. Conclusion

In this study, an additional surface coating on the additively manufactured carbon fiber reinforced Polyphenylene Sulfide (PPS) composite to improve surface properties required for composite part manufacturing mold. A thin film liquid thermoset polymer coating with ceramic particles was successfully applied on the composite using liquid spray coating technique. The coated test specimen showed significantly increased surface abrasion resistance compared to the non-coated test specimen. The wear index which represented weight loss corresponding to the number of abrasion cycle of the coated test specimen was lower than the non-coated test specimen (89%). The coated test specimen even had a lower wear index than traditional metals, aluminum 6061 T-6, and 1020 steel. The coated test specimen showed decreased static (40%) and kinetic (38%) friction coefficient compared to the non-coated test specimen. Also, the coated surface showed significantly improved vacuum integrated surface compared to the non-coated surface (95% decreased vacuum loss). The coated tool showed decreased (53.2%) average maximum demolding force compared to the non-coated tool, and the average kinetic surface friction coefficient of the coated tool was lower (46.4%) than the non-coated tool. However, the surface hardness test result showed that the coated test specimen had lower (23%) hardness than the non-coated test specimen, and the surface roughness of the coated test specimen was not improved compared to the non-coated test specimen.

Even the coated surface did not show improvement compared to the non-coated surface in every surface property test, it provided some beneficial surface properties to the additively manufactured fiber reinforced polymer composite for composite part manufacturing mold application. The goal of this research was providing a guideline for surface property tests for composite mold, and how to evaluate the performance of the coating in the composite part manufacturing mold application. Further research is necessary to investigate how different coating material and different coating technique affect surface property of the composite.

References

[1] Mallick PK. Fiber-reinforced composites: materials, manufacturing, and design. CRC press; 2007.

[2] Sterkenburg R, Wang PH. Structural composites: Advanced composites in aviation. Weyers Cave, Virginia: Avotek; 2013.

[3] Shah Mohammadi M, Ghani M, Komeili M, Crawford B, Milani AS. The effect of manufacturing parameters on the surface roughness of glass fibre reinforced polymer moulds. Compos Part B Eng 2017;125:39–48. https://doi.org/10.1016/j.compositesb.2017.05.028.

[4] Martínez-Mateo I, Carrión-Vilches FJ, Sanes J, Bermúdez MD. Surface damage of mold steel and its influence on surface roughness of injection molded plastic parts. Wear 2011;271:2512–6. https://doi.org/10.1016/j.wear.2010.11.054.

[5] Campbell FC. Manufacturing Processes for Advanced Composites. Elsevier Inc.; 2003. https://doi.org/10.1016/B978-1-85617-415-2.X5000-X.

[6] Stewart R. Moldmaking for composite materials. Plast Eng 2009;65:16–23. https://doi.org/10.1002/j.1941-9635.2009.tb00421.x.

[7] Duty CE, Springfield RM. Evaluation of Additive Manufacturing for Composite Part Molds. ORNL Manuf Demonstr Facil Tech Collab Final Rep 2014:1–5. https://doi.org/10.2172/1221722.

[8] Sudbury TZ, Springfield R, Kunc V, Duty C. An assessment of additive manufactured molds for hand-laid fiber reinforced composites. Int J Adv Manuf Technol 2017;90:1659–64. https://doi.org/10.1007/s00170-016-9464-9.

[9] Sauerbier P, Anderson J, Gardner DJ. Surface Preparation and Treatment for Large-Scale 3D-Printed Composite Tooling Coating Adhesion. Coatings 2018;8:457.

[10] Hassen AA, Lindahl J, Chen X, Post B, Love L, Kunc V. Additive manufacturing of composite tooling using high temperature thermoplastic materials. SAMPE Conf. Proceedings, Long Beach, CA, May, 2016, p. 23–6.

[11] Collaboration T, Report F. Evaluation of Additive Manufacturing for Composite Part Molds. 2014. https://doi.org/https://doi.org/10.2172/1221722.

[12] Wang PH, Kim G, Sterkenburg R. Investigating the Effectiveness of a 3D Printed

Composite Mold. Int J Aerosp Mech Eng 2019;13:684–8.

[13] Barocio E. Fusion Bonding of Fiber Reinforced Semi-crystalline Polymers in Extrusion Deposition Additive Manufacturing. Purdue University Graduate School, 2020.

[14] Hassen AA, Springfield R, Lindahl J, Post B, Love L, Duty C, et al. The durability of large-scale additive manufacturing composite molds. CAMX 2016 2016:26–9.

[15] Chardon G, Chanal H, Duc E, Garnier T. Study of surface finish of fiber-reinforced composite molds. Proc Inst Mech Eng Part B J Eng Manuf 2017;231:576–87. https://doi.org/10.1177/0954405415617929.

[16] Omar F, Brousseau E, Elkaseer A, Kolew A, Prokopovich P, Dimov S. Development and experimental validation of an analytical model to predict the demoulding force in hot embossing. J Micromechanics Microengineering 2014;24:55007.

[17] Delaney KD, Bissacco G, Kennedy D. A structured review and classification of demolding issues and proven solutions. Int Polym Process 2012;27:77–90.

[18] Post BK, Richardson B, Lind R, Love LJ, Lloyd P, Kunc V, et al. Big area additive manufacturing application in wind turbine molds. Solid Free Fabr 2017 Proc 28th Annu Int Solid Free Fabr Symp - An Addit Manuf Conf SFF 2017 2020:2430–46.

[19] Gombos ZJ, Summerscales J. In-mould gel-coating for polymer composites. Compos Part A Appl Sci Manuf 2016;91:203–10.

[20] Ahmad, Abdullah MR, Kader ASA. Effect of the Gel Coat Composition on the Tensile Strength for Glass Fibre Reinforced Polyester Composites. Adv. Mater. Res., vol. 1125, 2015, p. 79–83.

[21] Hornbaker M, Keene L, Krawiec R, Wilken T. The basics of liquid and powder coatings. Fabr 2013;November 2.

[22] Jack Feng CX. Materials processing and manufacturing methods. Elsevier; 2004. https://doi.org/10.1201/9781420039870.ch185.

[23] Hollaway LC. Handbook of polymer composites for engineers. Woodhead publishing; 1994.

[24] ASTM. Standard Test Method for Indentation Hardness of Aluminum Alloys by Means of a Barcol Impressor. vol. 27. 2010.

[25] ASTM International. ASTM D7127: Measurement of Surface Roughness of Abrasive Blast Cleaned Metal Surfaces Using a Portable Stylus Instrument. 2013.

[26] Silva F, Martinho R, Andrade M, Baptista A, Alexandre R. Improving the Wear Resistance of Moulds for the Injection of Glass Fibre–Reinforced Plastics Using PVD Coatings: A Comparative Study. Coatings (Basel) 2017;7:28.

[27] ASTM. ASTM D 4060-10: Standard Test Method for Abrasion Resistance of Organic Coatings by the Taber. 2010.

[28] Correia MS, Miranda AS, Oliveira MC, Capela CA, Pouzada AS. Analysis of friction in

the ejection of thermoplastic mouldings. Int J Adv Manuf Technol 2012;59:977–86.

[29] ASTM International. ASTM D5687-20: Standard guide for preparation of flat composite panels with processing guidelines for specimen preparation. 2020.

[30] Chailly M l, Gilbert V, Charmeau J-Y, Bereaux Y. Study of the Influence of Surface Mold Deposits on the Demolding Stage of the Injection Molding Process of Thermoplastics. ASME Int. Mech. Eng. Congr. Expo., vol. 47705, 2006, p. 879–85.

[31] Worgull M, Heckele MP, Hétu JF, Kabanemi KK. Modeling and optimization of the hot embossing process for micro-and nanocomponent fabrication. J Micro/Nanolithography, MEMS, MOEMS 2006;5:11005.

[32] Kinsella ME. Ejection forces and static friction coefficients for rapid tooled injection mold inserts. The Ohio State University, 2004.

[33] Davim JP. Tribology for engineers: A practical guide. Elsevier; 2011.